Customization of Platelet Rich Plasma via Avastin Conjugated Bead Technology

A Senior Thesis Presented to
The Faculty of the Department of Molecular Biology,
Colorado College

By
Imali Kegode

Prof. Sara Hanson
Primary Thesis Advisor

Prof. Darrell Killian
Secondary Thesis Advisor

Abstract

Platelet rich plasma (PRP) is a popular autologous therapy in clinic for tissue repair. Upon activation, platelets produce growth factors, which aid in tissue regeneration. However, previous literature shows that vascular endothelial growth factor (VEGF) can be detrimental to cartilage repair and regeneration due to the avascular nature of the tissue. Removal of VEGF from PRP via Avastin conjugated magnetic beads has been shown to promote improved cartilage formation. However, removal of VEGF via the VEGF inhibitor, Avastin, can produce adverse side effects if the dose is dispensed incorrectly or if it is delivered to patients who do not require the chemotherapeutic drug. Thus, we aim to investigate whether VEGF removal in PRP via Avastin conjugated magnetic beads promotes chondrogenesis of the chondrogenic mouse cell line, ATDC5. In this study, Avastin (Bevacizumab) is conjugated to Dynabeads™ M-270 Epoxy beads using the Dynabeads™ Antibody Coupling Kit. The beads were used to treat activated human PRP samples. VEGF and TGF-β ELISAs were utilized to analyze the concentration of growth factors before and after bead treatment. *In vitro* ATDC5 experiments were conducted to determine PRPs' effect on inducing chondrogenesis before and after treatment of VEGF removal. Our study suggests that the Avastin conjugated magnetic beads can selectively remove VEGF from PRP and, additionally, that the PRP with removed VEGF promotes the upregulation of key chondrogenesis factors such as Collagen 2 (*Col2a1*), while key hypertrophic cartilage factors such as Alp and VEGF are downregulated. Moreover, our research shows that Avastin conjugated beads can successfully and specifically remove VEGF from patient PRP samples. This proof-of-concept investigation shows that this technology could be used to remove specific growth factors, such as VEGF, in order to create specialized PRP therapies. Further investigation is needed using a more effective chondrogenesis model such as bone marrow-derived mesenchymal stem cells (BMSCs) or animal models.

Introduction

Cartilage is a flexible connective tissue that plays an important role in maintaining joint fluidity by cushioning the bones against impact (Karuppal, 2017). There are three major types of cartilage: hyaline, fibrous, and elastic (Chen, Fu, Wu, & Pei, 2017). Hyaline cartilage is the most widespread cartilage type and forms an articular surface throughout long bones and joint surfaces (Figure 1). Unlike other tissues, synthesized cartilage is not composed of lymphatics, nerves, or blood vessels. The tissue relies on diffusion of nutrients from capillaries in perichondrium (adjacent connective tissue) or from synovial fluid in joint cavities. Cartilage is comprised of a dense extracellular matrix (ECM) (Sophia Fox, Bedi, & Rodeo, 2009a), which are synthesized by chondrocytes. Chondrocytes synthesize the ECM, which is composed of water, collagen, proteoglycans, and non-collagen proteins (Lewis et al., 2006). Aggrecan is the primary cartilage-specific proteoglycan, and the collagen is primarily type II collagen, which interacts to form large fibrils that trap the aggrecan (Lewis, McCarty, Kang, & Cole, 2006). Overall, these components work together to retain water within the ECM which is critical to maintaining the structure and mechanical properties of cartilage (Sophia Fox, Bedi, & Rodeo, 2009b).

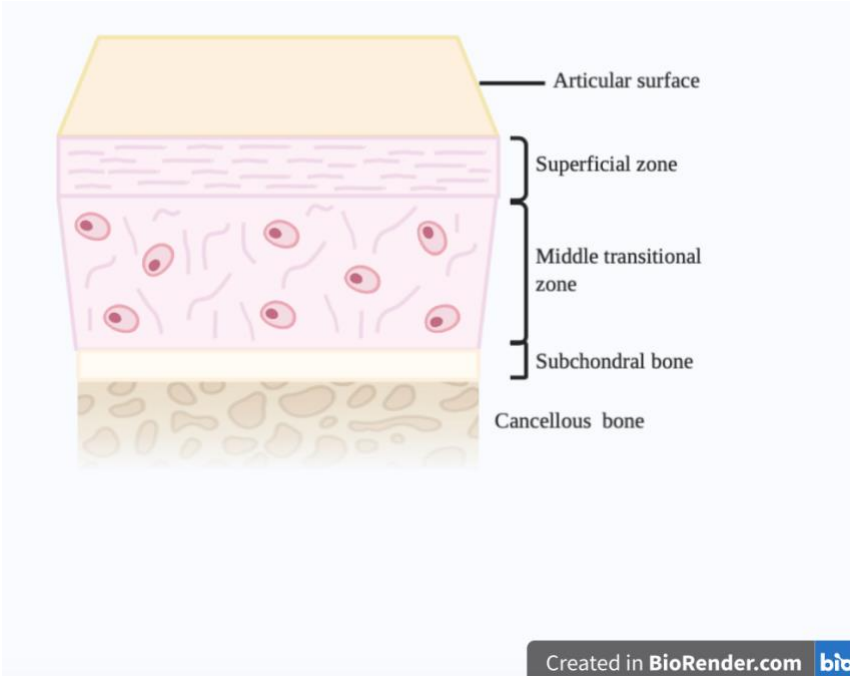

Figure 1. Hyaline cartilage structure. Basic schematic of hyaline cartilage architecture. Chondrocytes (pink cells) and collagen (light pink lines) are packed together in the middle transitional zone. Collagen and chondrocytes are packed tightly in the superficial zone. Figure created using BioRender.com

Cartilage is an avascular tissue with limited healing potential

The complex nature of cartilage can be attributed to its avascularity, which is due to the harsh biomechanical environment that the tissue endures (Sophia Fox et al., 2009).The ECM of cartilage contains non-collagen proteins such as thrombospondin-1, chondromodulin-1, type XVIII-derived endostatin, SPARC (secreted protein acidic and rich in cysteine), and type II collagen derived N-terminal pro peptide that have demonstrated antiangiogenic properties (Patra & Sandell, 2012). For example, thrombospondin-1 (TSP-1) is a cartilage matrix protein that has antiangiogenic properties (Patra & Sandell, 2012). In Gelse et al. 2012, the research investigated the effects of overexpressing TSP-1 within the joints of rat models. The study found that the over expression of TSP-1 in microfracture holes within the rat joints prevented ossification of the damaged cartilage tissue (Gelse et al., 2011). In a previous study by Bornstein 2009, showed that TSP-1 has strong anti-angiogenic effects due to the protein's interaction with CD36 receptors on endothelial cells that induce proapoptotic effects, thus interfering with VEGF signaling (Bornstein, 2009). Moreover, the presence of these non-collogen proteins work together to create an antiangiogenic barrier that contributes to the avascular property of cartilage.

This unique trait contributes to the limited healing potential of cartilage (Ramezanifard, Kabiri, & Hanaee Ahvaz, 2017). When the avascular properties of cartilage are broken down, vascular invasion occurs resulting in endochondral ossification (Patra & Sandell, 2012). During injury, inflammatory cytokines initiate the synthesis of collagen X, which plays a role in the calcification of cartilage during endochondral ossification (Fenwick, Gregg, & Rooney, 1999). For example, interleukin-1 (IL-1), interleukin-6 (IL-6), and tumor necrosis factor alpha (TNF-α) are inflammatory factors involved in osteoarthritis (OA) (Kennedy, Whitney, Evans, & LaPrade, 2018). Elevated levels of IL-1, TNF-α and IL-6 promote the synthesis of matrix

metalloproteinases (MMPs), which cause degradation of the collagenous framework and induce type X collagen expression by chondrocytes (Kennedy et al., 2018). The increase in type X collagen inhibits the production and secretion of the desired type II collagen (Kennedy et al., 2018). These pro-inflammatory factors also work to stimulate reactive oxygen species (ROS) and activate catabolic and degenerative factors that break down the architecture of the cartilage (Figure 2). Moreover, this irregular healing can result in the overproduction of type I and type X collagen and fibrocartilaginous tissue instead of the desired healthy cartilage (Richter, Schenck, Wascher, & Treme, 2015). This repair mechanism by the body results in fibrous tissue that is less stable than healthy cartilage and contributes to the advancement of degenerative osteoarthritis (Richter et al., 2015; Karuppal, 2017).

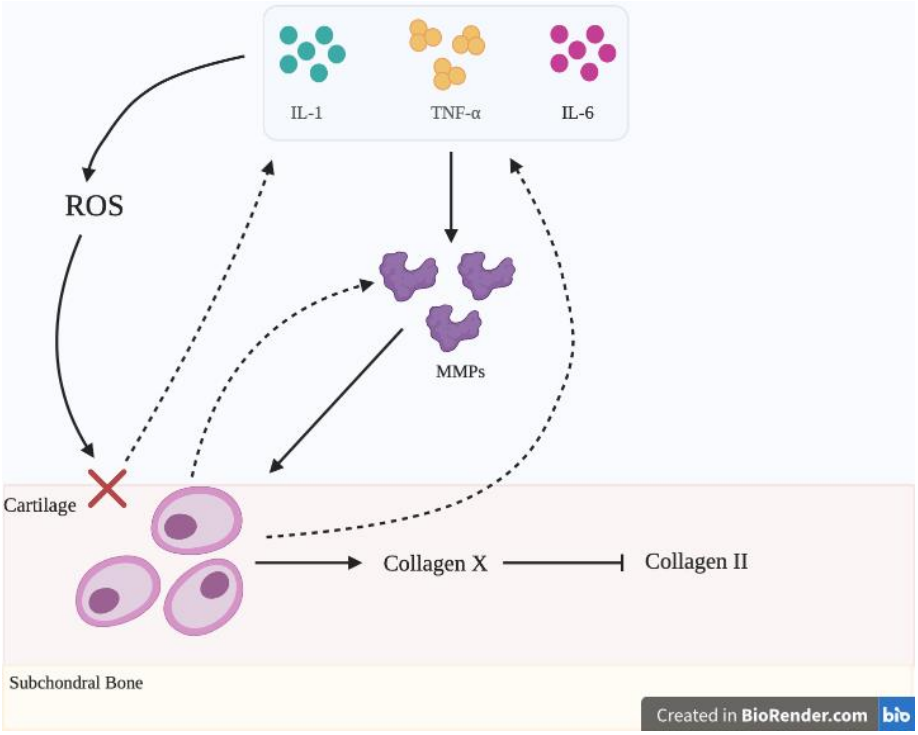

Figure 2. Molecular factors involved in OA. Interleukin-1 (IL-1, green), interleukin-6 (IL-6, maroon), and tumor necrosis factor alpha (TNF-a, yellow) are inflammatory factors involved in OA. The elevated levels of these cytokines induce the synthesis of matrix metalloproteinases (MMPs, purple). MMPs induce type X collagen expression by chondrocytes (pink). Type X collagen inhibits the production and secretion of the desired cartilage collagen, type II collagen. These pro-inflammatory factors stimulate

reactive oxygen species (ROS) causing the cartilage architecture to break down. ROS also initiates chondrocyte apoptosis. Figure modifiedfrom (Kennedy et al., 2018) and created using BioRender.com

Consequences of cartilage wound healing challenges on patient health

Osteoarthritis (OA) is a form of arthritis that results in inflammation or structural changes in the joints, ultimately causing pain and functionality issues (Cross et al., 2014) (Figure 3). Moreover, treatment of cartilage injuries is important in preventing the onset of osteoarthritis in patients. The goal for repairing such injuries is to regenerate tissue homeostasis. There are a variety of treatments used to resolve cartilage trauma and prevent fibrous tissue formation. Common surgical techniques include microfracture, autologous matrix-induced chondrogenesis, osteochondral autograft transfer, and autologous chondrocyte implantation. (Richter et al., 2015). These surgical techniques have been shown to produce some positive results in reducing the amount of fibrocartilaginous tissue, however, no single technique has been able to completely reproduce the healthy cartilage needed to prevent the onset of OA (Richter et al., 2015).

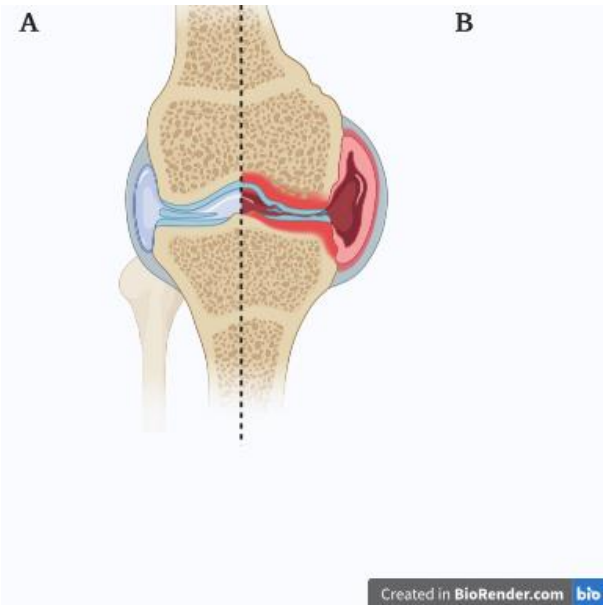

Figure 3. Cross section of a knee joint. A) Image of knee joint with healthy cartilage **B)** Image of knee joint with damage to the articular cartilage and increased swelling

around the joint. This is representative of an arthritic knee. Figure created using BioRender.com

Platelet rich plasma (PRP) therapies amplify natural growth factors to stimulate natural healing processes

Platelet rich plasma (PRP) is a volume of fractionated plasma from blood that contains platelet concentrate (Dhillon, Schwarz, & Maloney, 2012). PRP is collected from the patient's own blood through a series of centrifugation processes. In recent years, the use of PRP in conjunction with other surgical techniques has become a popular and common autologous therapeutic for tissue regeneration (Ramezanifard et al., 2017).To activate the PRP, a series of freeze thaw cycles are completed. Upon activation, PRP has a rich source of growth factors, produced by the elevated platelet levels, that are released into the surrounding cell environment to promote healing in the affected area (Kennedy et al., 2018). Platelets contain transforming growth factor- β (TGF-β), insulin-like growth factor, platelet-derived growth factor, vascular endothelial growth factor (VEGF), and epidermal growth factor, which all play a key role in tissue repair mechanisms (Dhillon et al., 2012). Injection of activated platelets to the site of injury initiates the body's repair mechanisms. For cartilage repair, TGF- β is a key growth factor because it stimulates the proliferation of mesenchymal stem cells (MSC) and ECM production (Dhillon et al., 2012). However, not all growth factors are beneficial for cartilage repair. Vascular endothelial growth factor (VEGF) initiates angiogenesis in the early stages of wound healing, which can be detrimental in the case of cartilage repair (Belair et al., 2016). Ramezanifard et al., investigated the consequences of PRP on MSC chondrogenesis. In this study, it was found that MSCs cultured with PRP secreted higher levels of VEGF then the other culture conditions (Ramezanifard et al., 2017). The presence of PRP in the MSC culture produced the upregulation and the expression of the hypertrophic marker Col-X, type X collagen, and the production of elevated calcium content and alkaline phosphatase activity (ALP) (Ramezanifard et al., 2017). These results suggest that the increased presence of VEGF in PRP influenced MSC cells to undergo endochondral ossification (Ramezanifard et al., 2017). Moreover, the avascular properties of cartilage tissue suggest that it is important to remove VEGF

from PRP in order to promote effective and healthy cartilage regeneration in affected patients.

Microsphere technology inefficiently sequesters VEGF from platelet rich plasma (PRP)

In 2015, Belair et al., attempted to sequester VEGF from PRP using VEGF-binding peptide conjugated microspheres technology (Belair et al., 2016). In this study, activated platelets were treated with PEG microspheres containing a VEGF-binding protein (VBP). ELISA analysis was used to determine the concentration of growth factors sequestered from the platelet concentrate (Belair et al., 2016). The results of this study showed that the microspheres technology was a novel tool to specifically sequester and regulate VEGF from human plasma (Belair et al., 2016). Although this strategy showed promising results, less than 20% of VEGF was able to be removed from the PRP samples (Belair et al., 2016). In an attempt to yield greater results, we modeled this study to determine if the use of magnetic beads (Dynabeads M-270 Epoxy) and the chemotherapy Avastin, a VEGF antagonist, were sufficient in sequestering VEGF from patient PRP. In this study, patient PRP samples were treated by incubation with the Avastin conjugated magnetic beads. After incubation, the beads were removed from the PRP samples via a magnet. The treated PRP samples were then used on ATDC5 cells, a chondrogenic cell line derived from mouse, for differentiation experiments. We hypothesize that VEGF removal in PRP by Avastin conjugated magnetic beads will promote chondrogenesis of ATDC5 cells. In this study we analyzed the success the Avastin conjugated beads have on removing VEGF from PRP and the effects these treated PRP sampled have on ATDC5 differentiation.

Methods

PRP preparation and activation

60mL of whole blood with anti-coagulant agent was collected from volunteer donors. Samples were centrifuged at 500g for 10 minutes using a Sorvall™ST 8 benchtop centrifuge (ThermoFisher Scientific, Waltham, MA). After centrifugation, the upper level of excess platelet poor plasma (PPP) was manually extracted. The

remaining leukocyte layer and top fraction of the red blood cell (RBC) layer was purposefully disrupted to release platelets that co-mingle in both layers. The plasma samples were transferred to 50 mL conical tubes and centrifuged again at 3000 g for 6 minutes. The supernatant consisting of excess leukocyte and plasma were extracted and discarded. The cell pellet was resuspended in the resulting 6 mL of PPP providing 6 mL of LP- PRP. The LP-PRP samples were produced at high to low concentrations of platelets (2,000K/µL to ~ 800K/µL). Platelet concentration was determined using CELL-DYN Ruby Hematology Analyzer according to manufacturer's instructions. Platelet rich plasma (PRP) was stored at -80°C until further use.

PRP was activated via freeze/thaw cycles before treatment with beads.

Avastin conjugation on magnetic beads

2.5mg of Dynabeads M-270 Epoxy was weighed out. Avastin solution was made with 1mg/mL of Avastin in Ultrapure water for a final concentration of 25µg/mL. Solution is centrifuged at 16,000g for 10 minutes at 4°C. Refer to Dynabeads™ Co-Immunoprecipitation Kit (Invitrogen™) for needed reagents. Beads were washed with C1 solution and put on magnet for 1 minute. Supernatant was removed. Avastin antibody and of C1 solution were added 1:1 to wash the beads. C2 solution was added, and the beads were incubated on a roller overnight at 37°C.

Tube was placed on magnet for 1 minute after incubation. Supernatant was removed and a series of washes were conducted. The tube was placed on the magnet in between each wash and supernatant was removed. Avastin beads were suspended in SB solution for a final concentration of 10mg/mL. The tube was stored at 4°C until use.

VEGF and TGF-β ELISAs

VEGF ELISA was performed using Human VEGF Quantikine ELISA Kit Procedure (R&D Systems) according to manufacturer’s instructions. The absorbance was read at 450nm with a reference set to 540nm or 570nm.

TGF-β ELISA was performed using TBF beta-1 Human/Mouse Uncoated ELISA Kit with Plates Procedure (Invitrogen) according to manufacturer's instructions. The absorbance was read at 450nm with a reference at 570nm.

Presto Blue Analysis

Media was removed room the cells and washed with PBS. Presto Blue and cell culture media were combined in a 1/10 solution. Presto Blue and media solution were added to cell wells and incubated for 2 hours at 37°C. Fluorescence was read at 570nm with 600nm reference wavelength.

ATDC5 Differentiation Treatment

ATDC5 cells were treated with chondrogenic media (DMEM-F:12, 1% penicillin-streptomycin, 10ng/mL TGF-β3, 100nM Dexamethasone, 50 µg/mL ascorbic acid 2-phosphate, 1mM sodium pyruvate, 40µg/mL proline, 6.25 µg/mL insulin, 6.25 µg/mL transferrin, and 6.25 µg/mL selenous acid) with 5% FBS for controls and varying percentages of activated treated or untreated PRP for the treated groups. Media was filtered with 0.45 µm Puradisc syringe filter (Whatman®, Sigma-Aldrich). Cells grew at 37°C and media was changed every two days until cells reached 100% confluency.

ATDC5 RNA Isolation

RNA isolation was performed using TRIzol™ RNA Isolation Reagents Protocol (ThermoFisher Scientific, Invitrogen) according to manufacturer's instructions. For RNA wash, samples were centrifuged at 12,000 xg at 4°C.

Real-Time PCR (qRT-PCR)

Primer sequences are demonstrated in Table 1. qPT-PCR analysis was performed according to qScript® cDNA SuperMix procedure (Quantabio) for cDNA synthesis methods.

For qRT-PCR data, cDNA samples (25ng) were mixed with SYBR green, Forward and Reverse primers (2µm), and RNase free water for a final volume of 15 µL per well. Samples were read on StepOnePlus™ Real-Time PCR System (Applied

Biosystems™, ThermoFisher Scientific) on the Fast SYBR® Green Master Mix setting. Holding stage: 95°C for 20 minutes, Cycling Stage: 95°C 3 minutes and 60°C for 30 minutes (40 cycles), and melt curve stage: 95°C for 15 minutes, 60°C for 1 hour, and 95°C for 15 minutes. ΔΔCt was used to normalize the expression of each gene against *Hprt*.

Results

Avastin conjugated magnetic beads are successfully made to effectively and specifically remove VEGF from PRP

The VEGF conjugate Avastin was conjugated to the Dynabeads M-270 Epoxy magnetic beads. The successfulness of conjugating Avastin to the magnetic beads was determined using an Avastin ELISA. For this experiment the supernatant from each wash step during bead preparation was used to test the amount of unbound Avastin in the solution. It was found that any unbound Avastin was removed from the beads after the second wash step of the bead preparation (Figure 4). Thus, it is determined that the bead preparation procedure is sufficient in removing any unbound Avastin. This indicates that we can treat the PRP with the Avastin conjugated beads without concern that any unbound Avastin is introduced into the patient PRP samples.

Since the bead preparation is sufficient, the beads were used to treat the patient PRP samples in order to determine if the beads can specifically sequester VEGF. To determine the efficiency of the Avastin conjugated magnetic beads, a VEGF enzyme-linked immunosorbent assay (ELISA) was performed. In this experiment, the Avastin conjugated beads were made in triplicate, all at a final concentration of 10mg/mL, and tested on each of the five PRP samples from volunteer donors for 2 hours at 37°C. The remaining PRP for each sample was used as an untreated control. As seen in Figure 5A, each of the untreated patient PRP samples had varying starting concentrations of VEGF. Despite the varying concentrations, the beads were able to remove over 90% of VEGF from each sample (Figure 5B). Therefore, it can be concluded that the beads work in removing over 90% of VEGF in PRP samples independent of initial physiological VEGF concentration. Since the beads were made and tested in triplicate, we combined removal data for each bead group and determined that VEGF removal for

each group was consistent (Figure 5C). Moreover, this data indicates that the Avastin conjugated beads were able to effectively remove the majority of VEGF from each treated PRP sample.

VEGF removal was determined by performing a TGF-β ELISA. Three of the treated PRP samples were used for this experiment. TGF-β is a growth factor that is desired in these customized PRP samples (VEGF- depleted PRP). From this experiment it was determined that after treatment with the beads there was no change in the TGF-β concentration each of the PRP samples, since there was no significant change in concentration before and after treatment with the beads (Figure 6). In conclusion, this data determines that the Avastin conjugated beads can specifically remove more that 90% of VEGF from PRP samples.

Lower percentage of VEGF- depleted PRP produces greatest ATDC5 cell proliferation results

For this experimentation, ATDC5 cell line was used. ATDC5 cells are derived from mouse teratocarcinoma cells and were used because they are characterized as a chondrogenic cell line (Yao & Wang, 2013). Before we can test PRP's effects on ATDC5 cell differentiation, we needed to determine the ideal percentage of PRP needed to maintain efficient cell proliferation (cell proliferation is not inhibited). For this experiment, cells were grown on 12-well tissue culture plates with ATDC5 growth medium for 24 hours after initial seeding. After this incubation, the cells were treated with filtered DMEM-F:12, 1% Penicillin-Streptomycin, and varying percentages of treated and untreated PRP (Figure 7). Cells were treated with the PRP medium for 48 hours. After this incubation Presto Blue was added to the cells in order to determine cell viability. The cells incubated with solution at 37°C for 2 hours. The Presto Blue solution was collected, and absorbance was read at 570nm with 600nm reference. This data suggests that the media with FBS and PRP and a higher PRP percentage produced little to no proliferation, which may be due to the high protein content found in the sample (Figure 7). It also shows that the media with the lower PRP percentages (1.25% and 2.5%) produced the better proliferation data since the results were close to our positive control, 10% FBS in normal ATDC5 growth media (Figure 7). Based on these

results, we performed a similar experiment with Avastin treated PRP percentages (Figure 8). All the PRP in this experiment was treated with the Avastin Conjugated beads. Presto Blue analysis was used again, and the data suggested that 3% and 4% treated PRP produced similar amounts of cell proliferation as our 10% FBS control (Figure 9). Moreover, we have determined that 3% or 4% treated PRP (VEGF-depleted) is the ideal percentage of PRP needed to maintain efficient cell proliferation. Based on these results we can design an ATDC5 differentiation experiment with the appropriate amount of PRP needed to maintain and promote cell proliferation.

Chondrogenic media treated with customized PRP upregulates chondrocyte specific genes in ATDC5 cells

In order to determine the customized PRP (VEGF-depleted) effects on the promotion of chondrogenesis, ATDC5 cells were treated with chondrogenic media and 4% treated or untreated PRP. Cells grew in a 12-well tissue culture plate with this media for 48 hours. TRIzol reagent was used to lyse cells for RNA isolation. After RNA isolation, qRT-PCR was used to determine if chondrocyte-specific or endochondral ossification-specific genes are being upregulated (Table 1). Three genes were analyzed, *Alp*, *Vegf*, and *Col2a1. A*lpis an endochondral ossification specific gene that plays a role in the growth and development of bones and teeth. *Vegf* is another endochondral ossification specific gene that induces the migration of vascular endothelial cells which is essential for bone growth and detrimental for avascular tissue like cartilage. *Col2a1* is a chondrocyte specific gene that is responsible for making a component of the pro-alpha1 (II) chain of type II collagen. If ATDC5 cells are undergoing chondrogenesis, it is expected that endochondral ossification specific genes such *as Vegf* and *Alp* are downregulated while chondrocyte specific genes, such as *Col2* are upregulated in the cells. There was an upregulation of Col2 in the cells that were treated with PRP without VEGF and a down regulation in Alp and VEGF (Figure 10). Using the ΔΔCt method, gene expression was normalized against the reference gene *HPRT*. Moreover, the qt-PCR data shows that the customized PRP (VEGF-depleted) does promote chondrogenesis in ATDC5 cells

Figures

Table 1. Primer Sequences

Primer	Forward Sequence	Reverse Sequence
Hprt	3’-CTGGTGAAAAGGACCTCTCGAA-5’	5’-CTGAAGTACTCATTATAGTCAAGGGCAT-3’
Ppia	3’-CGCGTCTCCTTCGAGCTGTTTG-5’	5’-TGTAAAGTCACCACCCTGGCACAT-3’
Col2a1	3’-AGGGCAACAGCAGGTTCACATAC-5’	5’-TGTCCACACCAAATTCCTGTTCA-3’
Agn	3’-AGTGGATCGGTCTGAATGACAGG-5’	5’-AGAAGTTGTCAGGCTGGTTTGGA-3’
Alp	3’-TGCCTACTTGTGTGGCGTGAA-5’	5’-TCACCCGAGTGGTAGTCACAATG-3’
ColX	3’-TTCTGCTGCTAATGTTCTTGACC-5’	5’-GGGATGAAGTATTGTGTCTTGGG-3’
Oc	3’-AGCAGCTTGGCCCAGACCTA-5’	5’-TAGCGCCGGAGTCTGTTCACTAC-3’
Vegf	3’-ACGCATTCCCGGGCAGGTGAC-5’	5’-TCTTCCGGGCTTGGCGATTTAG-3’

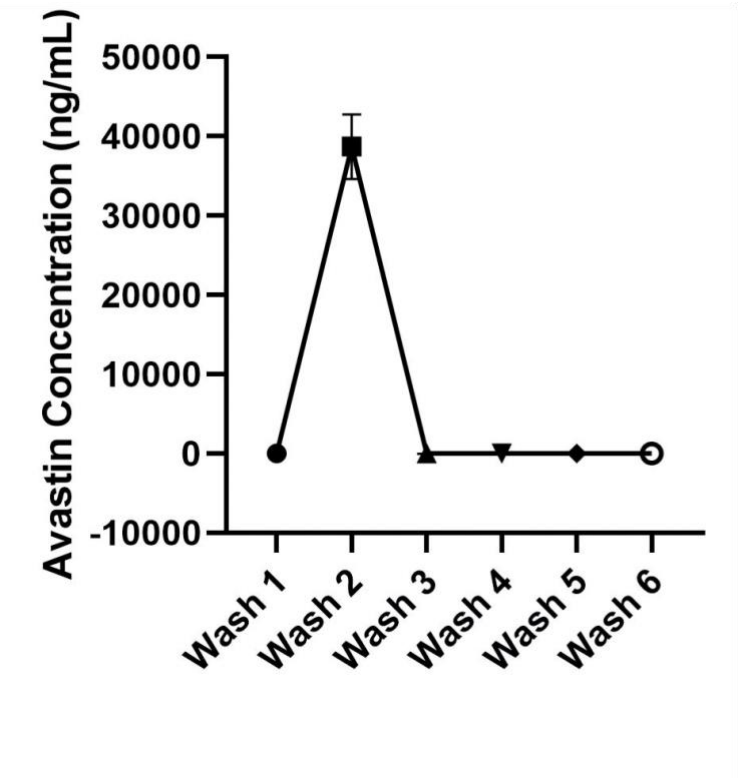

Figure 4. Bead preparation sufficiently removes unbound Avastin. Concentration determined by testing supernatant from each wash step during bead preparation with an Avastin ELISA**.**

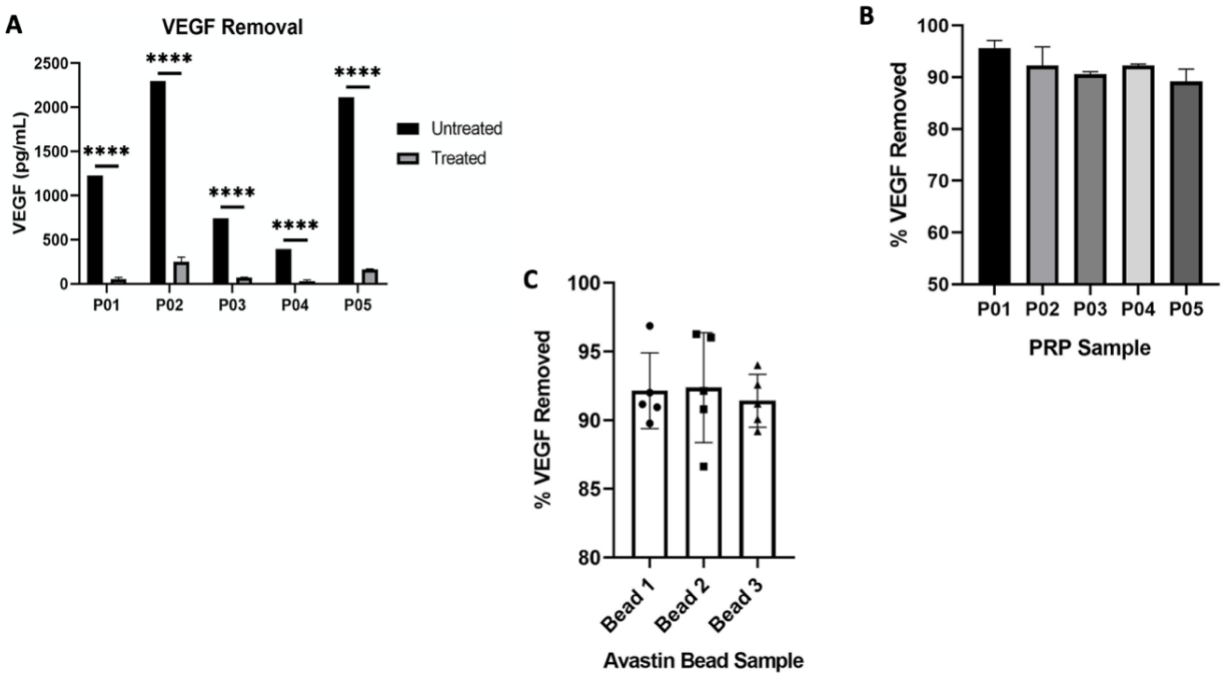

Figure 5. Avastin conjugated beads remove VEGF from PRP. Patient PRP samples were treated with Avastin conjugated beads for 2 hrs. at 37ºC. VEGF concentration was determined using a VEGF ELISA **A)** PRP treated with Avastin conjugated magnetic beads (Grey) and untreated PRP (Black). **B)** Percent of VEGF removed from treated PRP samples. **C)** Avastin beads were made in triplicate and tested on each sample. (**** = p <0.0001).

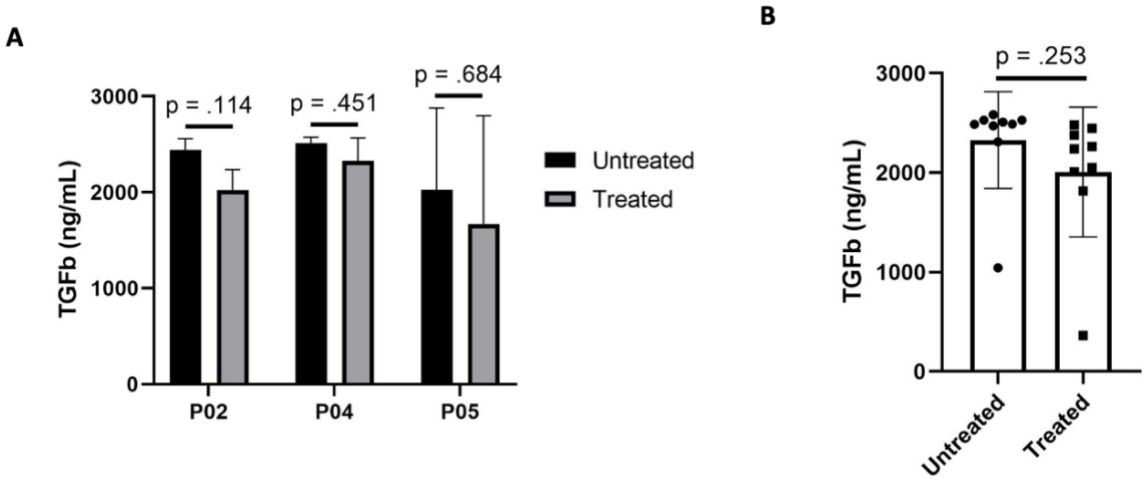

Figure 6. Avastin conjugated magnetic beads specifically removed VEGF from PRP. A) TGF-β concentration was determined using a TGF-β ELISA on three treated patient PRP samples. **B)** Untreated and treated data combined, respectively. One-way ANOVA test utilized. No significant difference ($p > 0.05$).

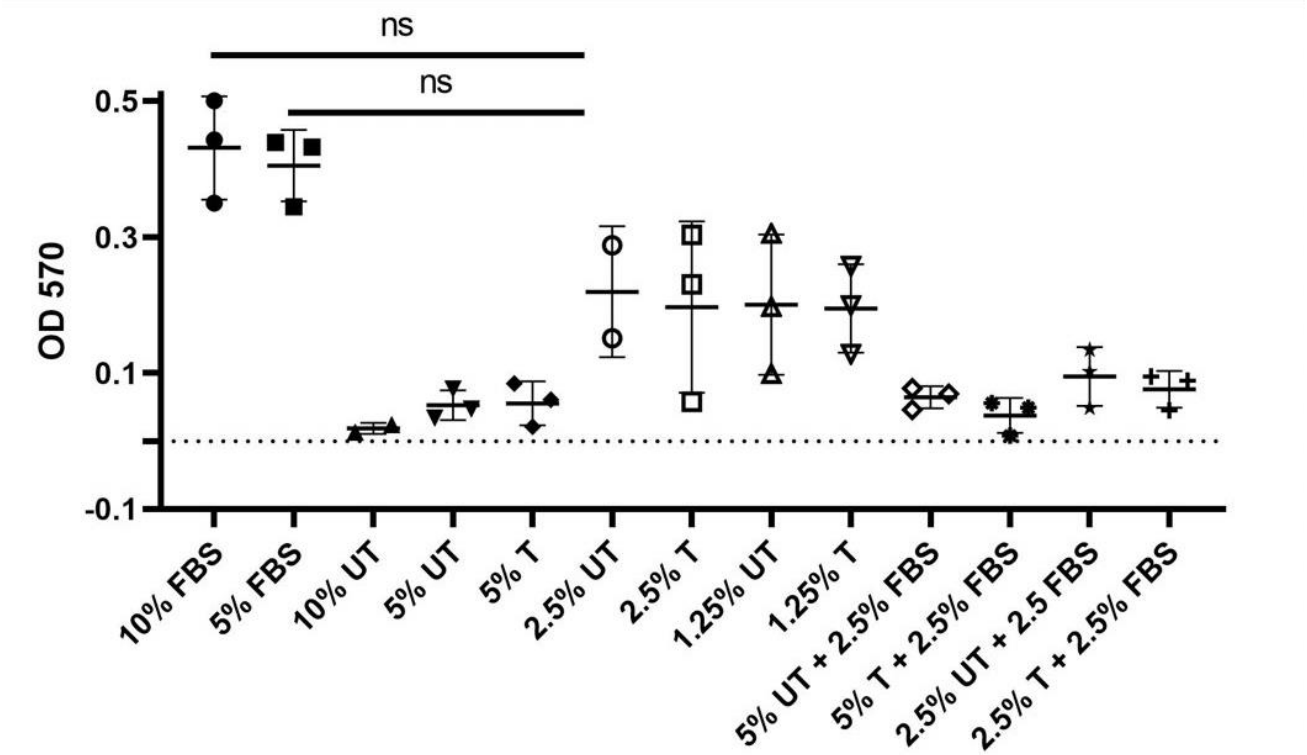

Figure 7. ATDC5 cells proliferate with lower percentage of PRP. Proliferation is determined by Presto Blue analysis. ATDC5 cells were grown in culture with DMEM F-12, 1% penicillin-streptomycin, and untreated or treated PRP for 48 hours. Presto Blue analysis was used to determine ATDC5 cell proliferation (One-way ANOVA, ns= no significance).

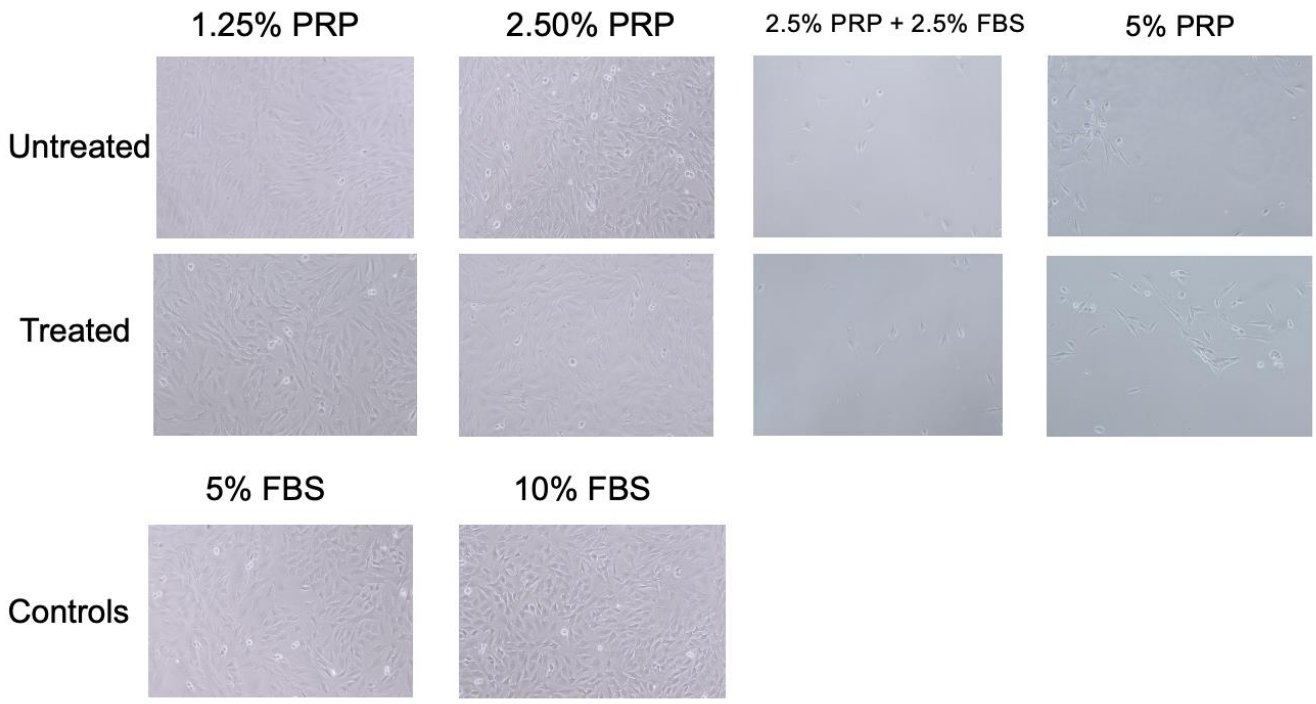

Figure 8. ATDC5 Cells Proliferate with a lower percentage of PRP and no FBS. Cells were grown in DMEM F-12, 1% Penicillin- Streptomycin, with or without FBS and varying percentages of treated PRP for 48 hours. Presto Blue analysis was used to determine ATDC5 cell proliferation.

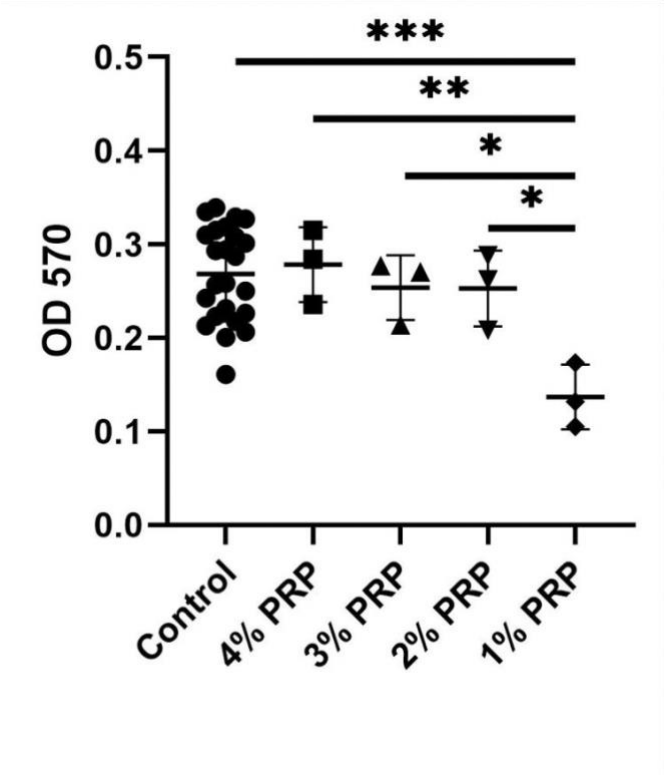

Figure 9. Lower percentage of PRP allows for cell proliferation. Cells were grown in DMEM F-12, 1% Penicillin- Streptomycin, 10ng/mL TGF-β3, 100nM Dexamethasone, 50 µg/mL ascorbic acid 2-phosphate, 1mM sodium pyruvate, 40µg/mL proline, 6.25 µg/mL insulin, 6.25 µg/mL transferrin, and 6.25 µg/mL selenous acid and varying percentages of treated PRP for 48 hours. Presto Blue analysis was used to determine ATDC5 cell proliferation. Controls were ATDC5 cells grown in DMEM-F:12, 1% penicillin-streptomycin, 10ng/mL TGF-β3, 100nM Dexamethasone, 50 µg/mL ascorbic acid 2-phosphate, 1mM sodium pyruvate, 40µg/mL proline, 6.25 µg/mL insulin, 6.25 µg/mL transferrin, and 6.25 µg/mL selenous acid with 5% FBS. (One-way ANOVA, * = $p < 0.05$, ** = $p < 0.01$, *** = $p < 0.001$).

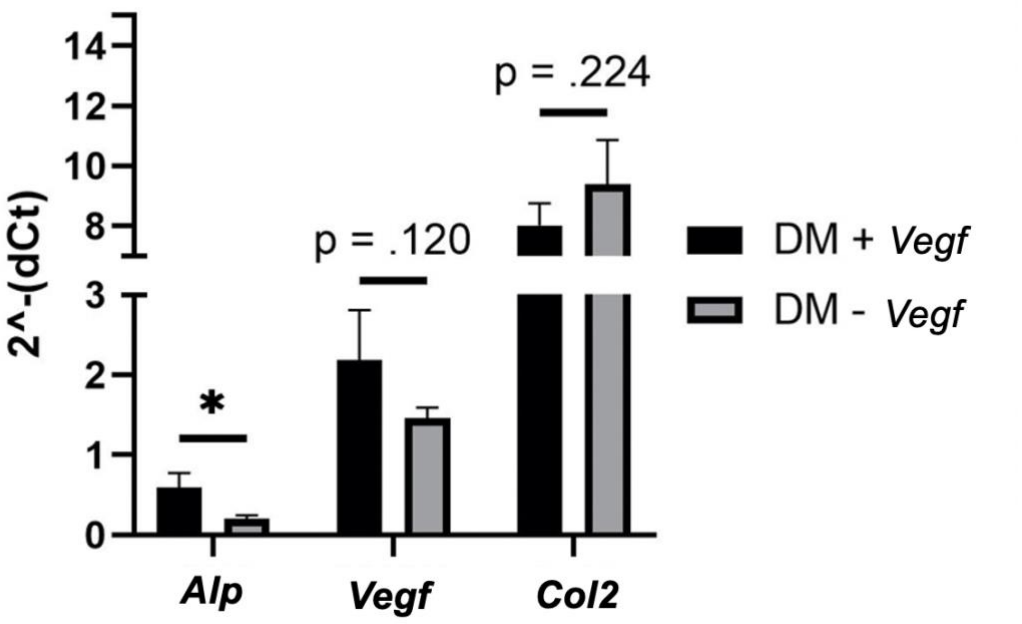

Figure 10. Expression level of chondrocyte specific and endochondral ossification related genes of ATDC5 cells. Cells were grown with differentiation media and treated or untreated PRP for 48 hours. Relative gene expression was determined by ΔΔCt calculations. (One-way ANOVA, * = $p < 0.05$).

Discussion

Avastin is used as a chemotherapy with harsh side effects, therefore, it is important that this drug is not introduced into the PRP after treatment. We found that the methods for conjugating Avastin to the magnetic beads (Dynabeads M-270 Epoxy), was sufficient in removing any unbound Avastin (Figure 4). In this study we found that the Avastin conjugated beads are able to specifically remove >90% of VEGF from patient PRP samples (Figures 5 and 6). This result was a substantial increase compared to Belair et al. 20% VEGF removal using microsphere technology (Belair et al., 2016). Moreover, the Avastin conjugated Dynabeads M-270 Epoxy technology proves to be a more sufficient tool to specifically remove VEGF from patient PRP samples. After determining that the Avastin conjugated beads were able to remove VEGF from PRP, we tested whether the treated PRP samples (PRP with VEGF removed) would be able to promote chondrogenesis of ATDC5 cells. It was found that a lower percentage of PRP without FBS helped promote ATDC5 cell proliferation (Figure 7 and 8). From this data, we then tested 4%- 1% PRP on the ATDC5 cells and found that the 4% PRP treatment produced results similar to that of the control (Figure 9). Moreover, these experiments revealed that 4% PRP treatment on ATDC5 cells promotes cell proliferation and therefore is not toxic to the cells. Based on these results we used 4% PRP to treat the ATDC5 cells with differentiation media to see if PRP with no VEGF (treated with the Avastin conjugated beads) was able to promote chondrogenesis. We ran a qRT-PCR to determine the expression levels of chondrogenic specific markers (Collagen II) and markers for hypertrophic differentiation *(Alp* and *Vegf*) in ATDC5 cells treated with differentiation media and PRP with or without VEGF. We found that *Alp* and *Vegf* were downregulated in cells that were treated with PRP without VEGF and collagen II was upregulated in these cells (Figure 10). Moreover, this data supports our hypothesis by showing that PRP treated with the Avastin conjugated beads promotes chondrogenesis in ATDC5 cells by upregulating chondrogenic specific markers like collagen II and downregulating hypertrophic differentiation markers such as *Vegf* and *Alp* that are involved with the onset of osteoarthritis.

The results of this study demonstrate that the antibody coupled magnetic bead technology is a sufficient tool to specifically remove VEGF from patient PRP samples

when compared to the VEGF- binding peptide conjugated microspheres technology used by Belair, et.al 2016 which was only able to sequester ~20% of VEGF from patient PRP samples. Therefore, this technology can be used to customize PRP by selectively removing specific growth factors and proteins to enhance the regenerative response in a variety of tissues treated. Before starting additional *in vitro* and *in vivo* models the affinity of Avastin to the magnetic beads should be measured in order to determine how much Avastin is needed to ensure that more than 90% of the VEGF is depleted from the PRP samples. This will help to prevent excess Avastin that could potentially result in a fraction of the chemotherapy to be present in the PRP after the bead washing procedures. The research used an ATDC5 cell line that is derived from mouse teratocarcinoma cells. The use of mouse cancer cells poses as a limitation for this study since they are prone to division compared to the native human chondrocytes. Therefore, to overcome this, future *ex vivo* experimentation with bone marrow stromal cells (BMSCs) and discarded chondyles should be used. Since this study was limited to *ex vivo* differentiation, in order to streamline these results further experimentation using animal models, such as mouse models, and discarded condyles should be used.

Acknowledgements

I would like to thank Dr. Johnny Huard and Dr. Sudheer Ruvari for giving me the opportunity to conduct this research at the Steadman Philippon Research Institute (SPRI) in Vail, Colorado. I would also like to acknowledge Michael Mullen for mentoring me during my time at SPRI and aiding in this research. I would also like to thank my thesis advisor, Dr. Sara Hanson for guiding and supporting me through my senior thesis process.

References

Andia, I. and Maffulli, N. (2013). Platelet-rich plasma for managing pain and inflammation in osteoarthritis. *Nature reviews. Rheumatology* 9, 721-730.

Belair, D. G., Miller, M. J., Wang, S., Darjatmoko, S. R., Binder, B. Y. K., Sheibani, N. and Murphy, W. L. (2016). Differential regulation of angiogenesis using degradable VEGF-binding microspheres. *Biomaterials* 93, 27-37.

Bornstein, P. (2009). Thrombospondins function as regulators of angiogenesis. *Journal of cell communication and signaling*3, 189-200.

Chen, S., Fu, P., Wu, H. and Pei, M. (2017). Meniscus, articular cartilage and nucleus pulposus: A comparative review of cartilage-like tissues in anatomy, development and function. *Cell Tissue Res* 370, 53-70.

Cross, M., Smith, E., Hoy, D., Nolte, S., Ackerman, I., Fransen, M., Bridgett, L., Williams, S., Guillemin, F., Hill, C. L. et al. (2014). The global burden of hip and knee osteoarthritis: Estimates from the global burden of disease 2010 study. *Annals of the Rheumatic Diseases* 73, 1323-1330.

Dhillon, R. S., Schwarz, E. M. and Maloney, M. D. (2012). Platelet-rich plasma therapy - future or trend? *Arthritis research & therapy* 14, 219.

Fenwick, S. A., Gregg, P. J. and Rooney, P. (1999). Osteoarthritic cartilage loses its ability to remain avascular. *Osteoarthritis and cartilage* 7, 441-452.

Filardo, G., Kon, E., Pereira Ruiz, M. T., Vaccaro, F., Guitaldi, R., Di Martino, A., Cenacchi, A., Fornasari, P. M. and Marcacci, M. (2011). Platelet-rich plasma intra-articular injections for cartilage degeneration and osteoarthritis: Single- versus double-spinning approach. *Knee Surg Sports Traumatol Arthrosc* 20, 2082-2091.

Gelse, K., Klinger, P., Koch, M., Surmann-Schmitt, C., von der Mark, K., Swoboda, B., Hennig, F. F. and Gusinde, J. (2011). Thrombospondin-1 prevents excessive ossification in cartilage repair tissue induced by osteogenic protein-1. *Tissue engineering. Part A* 17, 2101-2112.

Hamilton, J., Nagao, M., Levine, R. B., Chen, D., Olsen, R. B. and Im, H. (2016). Targeting VEGF and its receptors for the treatmentof osteoarthritis and associated pain

He, Y., Siebuhr, A. S., Brandt-Hansen, N. U., Wang, J., Su, D., Zheng, Q., Simonsen, O., Petersen, K. K., Arendt-Nielsen, L., Eskehave, T. et al. (2014). Type X collagen levels are elevated in serum from human osteoarthritis patients and associated with biomarkers of cartilage degradation and inflammation. *BMC musculoskeletal disorders* 15, 309.

Javad Parvizi and Gregory K. Kim. (2010). Chapter 39 - cartilage. In *High Yield Orthopaedics*, pp. 80-81: Elsevier Inc.

Karuppal, R., Dr. (2017). Current concepts in the articular cartilage repair and regeneration. *Journal of Orthopaedics* 14, A1-A3.

Kennedy, M. I., Whitney, K., Evans, T. and LaPrade, R. F. (2018). Platelet-rich plasma and cartilage repair. *Curr Rev Musculoskelet Med* 11, 573-582.

Lewis, P. B., McCarty, 3., L Pearce, Kang, R. W. and Cole, B. J. (2006). Basic science and treatment options for articular cartilage injuries. *The journal of orthopaedic and sports physical therapy* 36, 717-727.

Nagao, M., Hamilton, J. L., Kc, R., Berendsen, A. D., Duan, X., Cheong, C. W., Li, X., Im, H. and Olsen, B. R.(2017). Vascular endothelial growth factor in cartilage development and osteoarthritis. *Scientific reports* 7, 1-16.

NEWTON, P. T., STAINES, K. A., SPEVAK, L., BOSKEY, A. L., TEIXEIRA, C. C., MACRAE, V. E., CANFIELD, A. E. and FARQUHARSON, C. (2012). Chondrogenic ATDC5 cells: An optimised model for rapid and physiological matrix mineralisation. *International Journal of Molecular Medicine* 30, 1187-1193.

Patra, D. and Sandell, L. J. (2012). Antiangiogenic and anticancer molecules in cartilage. *Expert reviews in molecular medicine* 14, e10.

Ramezanifard, R., Kabiri, M. and Hanaee Ahvaz, H. (2017). Effects of platelet rich plasma and chondrocyte co-culture on MSC chondrogenesis, hypertrophy and pathological responses. 15.

Richter, D. L., Schenck, R. C., Wascher, D. C. and Treme, G. (2015). Knee articular cartilage repair and restoration techniques. *Sports health* 8, 153-160.

Sophia Fox, A. J., Bedi, A. and Rodeo, S. A. (2009). The basic science of articular cartilage: Structure, composition, and function. *Sports health* 1, 461-468.

Yao, Y. and Wang, Y. (2013a). ATDC5: An excellent in vitro model cell line for skeletal development. *Journal of cellular biochemistry* 114, 1223-1229.

Yao, Y. and Wang, Y. (2013b). ATDC5: An excellent in vitro model cell line for skeletal development. *Journal of cellular biochemistry* 114, 1223-1229.

Yao, Y., Zhai, Z. and Wang, Y. (2014). Evaluation of insulin medium or chondrogenic medium on proliferation and chondrogenesis of ATDC5 cells. *BioMed research international* 2014, 569241-8.